Renewable and Sustainable Energy Reviews 17 (2013) 216–227

Contents lists available at SciVerse ScienceDirect

Renewable and Sustainable Energy Reviews

journal homepage: www.elsevier.com/locate/rser

A current and future study on non-isolated DC–DC converters for photovoltaic applications

M.H. Taghvaee [a,*], M.A.M. Radzi [a], S.M. Moosavain [b], Hashim Hizam [a], M. Hamiruce Marhaban [a]

[a] Department of Electrical and Electronic Engineering, Faculty of Engineering, Universiti Putra Malaysia, 43400 Serdang, Selangor, Malaysia
[b] Department of Engineering, Shahrood Branch, Islamic Azad University, Shahrood, Iran

A R T I C L E I N F O

Article history:
Received 6 March 2012
Received in revised form
8 September 2012
Accepted 15 September 2012
Available online 23 October 2012

Keywords:
DC–DC converter
Photovoltaic (PV)
Maximum Power Point Tracking (MPPT)
Non-isolated
Topology
Efficiency

A B S T R A C T

Photovoltaic (PV) is a fast growing segment among renewable energy (RE) systems, whose development is owed to depleting fossil fuel and climate-changing environmental pollution. PV power output capacity, however, is still low and the associated costs still high, so efforts continue to develop PV converter and its controller, aiming for higher power-extracting efficiency and cost effectiveness. Different algorithms have been proposed for Maximum Power Point Tracking (MPPT). Since the choice of right converter for different application has an important influence in the optimum performance of the photovoltaic system, this paper reviews the state-of-the-art in research works on non-isolated DC–DC buck, boost, buck–boost, Cúk and SEPIC converters and their characteristics, to find a solution best suiting an application with Maximum Power Point Tracking. Review shows that there is a limitation in the system's performance according to the type of converter used. In can be concluded that the best selection of DC–DC converter which is really suitable and applicable in the PV system is the buck–boost DC–DC converter since it is capable of achieving optimal operation regardless of the load value with negotiable performance efficiency and price issue.

Contents

1. Introduction 216
2. Methods of measuring PV module *I–V* curves 218
3. DC–DC buck converter 218
4. DC–DC boost converter 219
5. Comparing characteristics of buck and boost converters 220
6. DC–DC buck-boost converter 221
7. Comparing buck, boost, and buck-boost converters 221
8. DC–DC cúk converter 222
9. DC–DC sepic converter 223
10. Comparing main types of non-isolated converters 223
11. Conclusion 225
References 225

1. Introduction

Climate change and the implications of its threats are the most challenging problems facing the world today [1]. The main reason for climate change is the burning of fossil fuels, which releases greenhouse gases (GHG). Almost 80% GHG are fossil-fuel-based. Meanwhile, world primary energy demand will have increased almost 60% between 2002 and 2030, averaging 1.7% increase annually, increasing still further the GHG [2]. Oil reserves would have been exhausted by 2040, natural gas by 2060, and coal by 2300 [3]. Electricity generation by RE sources is one way to overcome global warming and future energy shortage [4,5]. RE is in short, sustainable and clean energy sourced from nature [6].

PV is one of the more important sources of RE [7]. Its contribution to the world's energy portfolio is significant and will, by 2040, have contributed the most to electricity generation

* Corresponding author. Tel.: +60 3 89464470; fax: +60 3 89466327.
E-mail address: taghvaee.h@gmail.com (M.H. Taghvaee).

1364-0321/$ - see front matter © 2012 Elsevier Ltd. All rights reserved.
http://dx.doi.org/10.1016/j.rser.2012.09.023

among all RE candidates [8–10]. Its weakness, however, is its intermittent, variable, and non-linear nature (see Fig. 1). This causes issues of high per-kW installation cost but low efficiency in PV generators [11–13]. More research works that focus on how to extract more power more effectively from PV cells are needed. Two common such ways are sun-based tracking and MPPT [14,15]. Surveys show PV systems with sun tracking collecting 30%–40% more energy than does PV systems without sun tracking [16,17]. Directly connecting a PV module to the load enables extraction of 31% energy, which increases to 97% through use of MPPT [18,19].

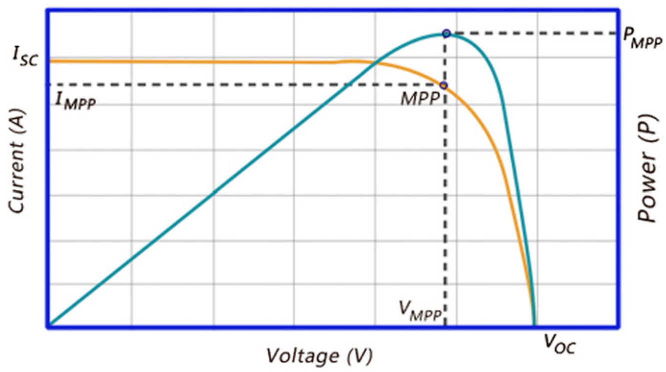

Fig. 1. Non-linear *I–V* and *P–V* curve characteristics of PV panel.

The maximum extractable power from PV panels depends not only on the strength of the solar irradiation but also on the operating point of the energy conversion system. MPPT is of paramount importance to the system as it not only maximizes system efficiency but also minimizes the return of investment on the PV installation [20]. To ensure maximum extraction of power, the maximum power point (MPP) should first be found before the system's operation point is driven to that point. A DC–DC converter will vary the apparent impedance R_i of a PV module to match with the R_{MPP} value. The action is as formulated in the last column of Table 1. Various MPPT algorithms are used for this, in various DC–DC converter topologies. Converters have two tasks: interface a PV panel and an RE source or the grid (or etc.), and drive the operating point of the PV panel to the MPP [21]. Converter configuration thus matters to optimal performance of a PV system. Fig. 2 is the block diagram of a PV system comprising MPPT and DC–DC converter.

Converters are divided into categories of application, types of switching, current modes, etc. Frequently-used terms for DC–DC

Table 1
Different non-isolated DC/DC converter and representation of input resistance versus duty cycle and conversion ratio.

Non-isolated DC–DC converters circuit diagrams	Input resistance curve versus duty cycle I	Voltage conversion ratios	Resistance conversion ratios
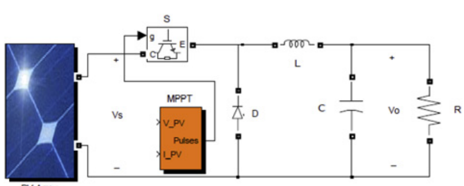	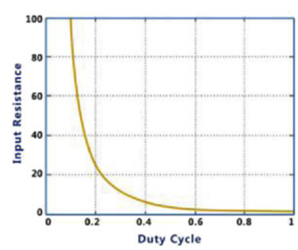	$\frac{Vo}{Vs}=D$	$Ri=\frac{Rl}{D^2}$
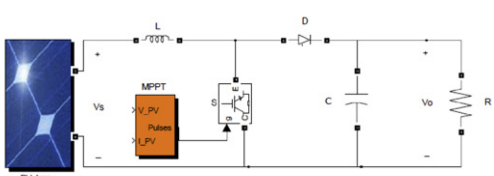	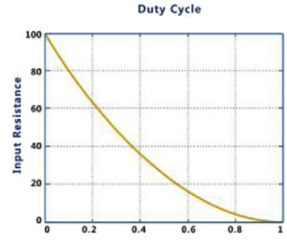	$\frac{Vo}{Vs}=\frac{1}{1-D}$	$Ri=(1-D)^2.Rl$
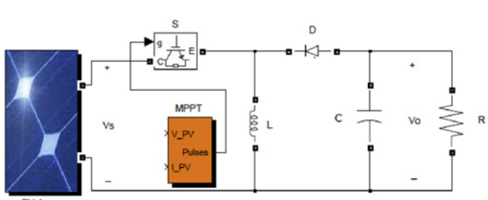		$\frac{Vo}{Vs}=\frac{D}{1-D}$	$Ri=\frac{(1-D)^2}{D^2}.Rl$
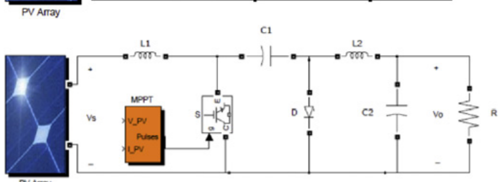		$\frac{Vo}{Vs}=-\frac{D}{1-D}$	$Ri=\frac{(1-D)^2}{D^2}.Rl$
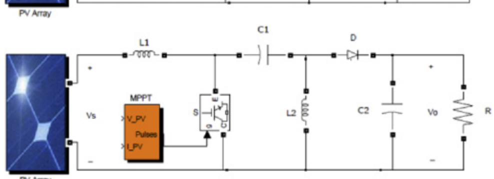		$\frac{Vo}{Vs}=\frac{D}{1-D}$	$Ri=\frac{(1-D)^2}{D^2}.Rl$

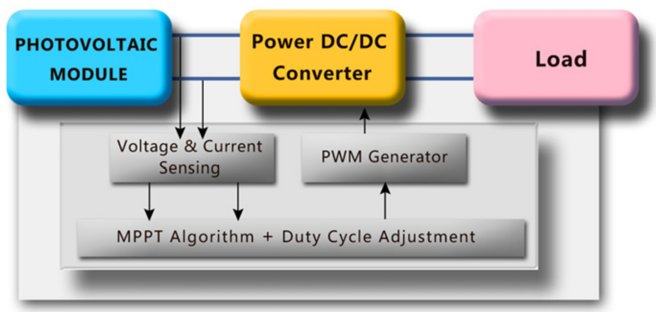

Fig. 2. PV panel with DC–DC converter and MPPT.

converter types are non-isolated and isolated. ''Isolation'' refers to the electrical barrier separating the input and the output of a DC–DC converter. This paper reviews the application of various non-isolated converter topologies used in PV systems.

Methods of extracting *I–V* curve will be introduced first before main topologies of non-isolated DC–DC converters (buck, boost, buck–boost, Cúk and Single Ended Primary Inductor Converter (SEPIC)) are reviewed. The review is categorized by converter topology, operational region, application, and advantages or disadvantages of the topologies. Each section will be addressed with a comparison of the converters. Conclusions will be drawn at the end of the paper.

2. Methods of measuring PV module *I–V* curves

Various instrumentation systems can be used to measure efficiency and other parameters of PV panels. Methods of extracting the *I–V* curves of PV panels have been reviewed.

One method is the capacitive method, which uses capacitor as load [22,23]. As capacitor charge increases, current drops and voltage rises. When charging completes, the current supplied by the PV panel becomes zero, achieving an open circuit.

Another method is the electronic-load method, which uses transistor as load. To trace the *I–V* curve of the module, a MOSFET must operate in its three modes of operation: cut-off, active, and ohmic [24,25].

Yet another method is the four-quadrant-power-supply method, which simulates DC output resources such as PV panels, fuel-cell stack, etc. [26–28].

Bipolar power amplifier method uses traditional power amplifiers (two BJT transistors) as load for forward and reverse currents [29,30].

The simplest method to measure PV current–voltage characteristic curve is through use of a variable resistor. For such measurement, it is the most popular method, focused on in this review.

In variable–resistor method, the resistor value is adjusted in steps from zero to infinity and from short circuit (full load) to open circuit. The voltage and the current in each step are measured, to obtain the current–voltage curve. Resistors for high powers are almost unavailable, so this method is applicable only to low-power stacks and modules [31].

The operating point of a load-connected PV generator is the point its characteristic curve intersects the load curve. This point sometimes is not the same as the PV generator's MPP, causing the PV generator to be not maximally efficient. In a unique case when both curves intercept each other exactly at MPP, the PV module output power is at the maximum.

Generation curve typically changes with radiation and temperature variations, whereas load curve depends on the type of load connected to the PV module. To ensure PV module operation point always at MPP, DC–DC converters are used [32].

Table 1 gives the non-isolated DC–DC converter circuit diagram, input resistance curve versus duty cycle *D*, the voltage conversion ratios for Continuous Current Mode (CCM), and the resistance conversion ratios.

3. DC–DC buck converter

In DC–DC buck converter or step-down converter, the output voltage magnitude is always lower than the input voltage magnitude [33,34], so this topology can be used for connecting high module voltages to low load or battery voltages.

PV apparent impedance R_i is converter input impedance. By changing the duty cycle *D*, R_i value can be matched with that of the optimum resistance R_{MPP}. Table 1 has the resistance conversion ratio of a buck converter. As *D* is in the interval [0,1], a buck converter cannot reflect impedances that are smaller than the load impedance and therefore does not achieve values that are near the short-circuit current I_{sc} of the PV module [35], i.e., a buck converter operates only with $R_{load} >= R_{mpp}$.

Fig. 3 shows that a buck converter does not allow tracing of PV *I–V* curve points that are close to I_{sc} and that when the buck converter is used as MPPT, the MPP will be tracked as if it is restricted to within the operation region.

General categories of buck converters are those that modulate the input voltage through PWM to generate the output voltage required for battery charging, and those that cause the PV panel to operate at the MPP. Most of the papers studied show common use of buck topology to track MPP and extract maximum power from PV panels [36–41].

Koutroulis et al. discussed an autonomous PV system that has a microcontroller-based DC–DC buck converter. The system is highly efficient, costs less, and can be simply adapted to energy sources such as wind turbine. The PV array output power directly controls the DC–DC buck, simplifying the converter. Experiment results show use of the proposed MPPT control increasing PV output power by as much as 15% when the DC–DC converter duty cycle is set so that the PV array produces maximum power at 1 kW/m^2 and 25 °C [42]. Chian-Song showed DC–DC buck converter regulating the output power of a standalone PV system via Takagi–Sugeno fuzzy approach to adjust the converter's duty cycle in generating the PWM signal switching the MOSFET. The frequency of the PWM signal was set to 100 KHz [43].

Chew and Siek presented standalone PV system for battery charging and fed the resistive load through use of single-inductor quad-input-dual-output (QIDO) DC–DC buck converter to reduce

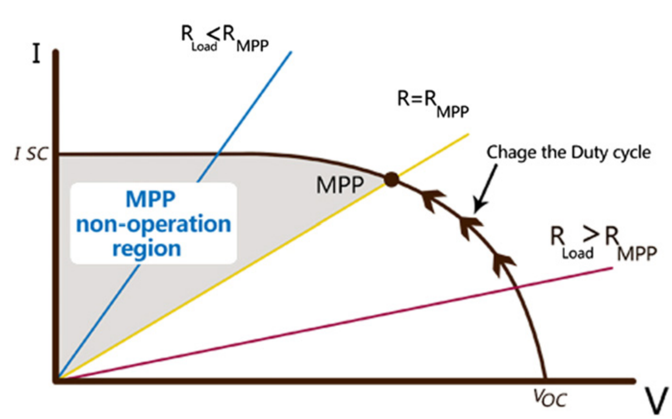

Fig. 3. Operational and non-operational regions of the *I–V* curve in buck DC–DC converters.

the number of components. QIDO can regulate three PV modules independently through four buck converters; each PV module can operate at its own MPP. This translates to 56.25% fewer components, reducing system cost and increasing system cost-efficiency, the percentage as compared with a system of four buck converters [44].

A new topology by Zhang et al. for MPPT controller with buck DC–DC converter for solar micro-grid applications has variable inductance. The inductance reduces with the increased current corresponding to increased incident solar irradiation. The method's advantages are the up to 75% smaller inductor, the stable step response to changes in the solar input, and the extended range of operation to low light levels and partial shading of the solar panels [45]. Veerachary proposed a novel fourth-order buck converter that tracks maximum PV power at all levels of solar insolation. As compared with conventional buck, the novel topology better reduces the source current ripple but has similar steady-state performance. Ripple is further reduced through use of a coupled inductor, which, for specific combinations of inductance and coupling coefficient not only reduces the core size but also improves converter performance through the reduced ripple. The coupled inductor of this topology also eliminated the problem of zeroes in the right half of the s-plane (RHP). Note that this paper presents MPPT operation of the load tracking region of a fourth-order buck converter [46] (see Fig. 3).

Yang et al. compared multiple-input converters instead of several single-input converters; the former has simpler circuits and cost less. They also proposed as MPPT, a one-cycle control of a double-input buck converter, to eliminate the interactions of the control loops and simplify the controller design. One-cycle control does not need a current regulator, and the design conditions of the output voltage regulator in various operating modes are the same [47]. Villalva et al. regulated PV panel output voltage through use of a buck DC–DC converter that interfaces the PV array and the load. The converter input voltage is controlled to regulate the array operating point. Besides reducing losses and stress through limited-bandwidth regulation of the converter duty cycle, control of the converter input voltage reduces settling time and avoids oscillation and overshoot, easing function of MPPT methods [48].

Perníá et al. presented a buck-topology standalone PV system. A controller connects the PV panels to 12 V or 24 V batteries so the converter operates at the PV panel MPP. The experiment results show the topology (buck with synchronous rectification) to theoretically increase efficiency to 95% [49].

Linear Current Booster (LCB) is an extended application of DC–DC buck converter. It is a special-purpose MPPT, designed to match PV array characteristics to those of dc motors, and was designed for daytime operations such as pumping, and especially for low illumination levels. LCB enables pumping of up to 20% more fluid [16].

Oi et al. investigated direct coupling between PV and water pump and considered the problem of starting a water pump in low irradiance. The LCB they used converted the low current and high voltage of the MPP into high-current and low-voltage power, satisfying pump motor characteristics [50].

4. DC–DC boost converter

In DC–DC boost or step-up converter, the output voltage magnitude is always higher than the input voltage magnitude [33], so this topology can be used to connect high load/battery voltages and low module voltages.

As is theorized of buck converter resistance conversion ratio, because the value of duty cycle is between [0,1], a boost converter

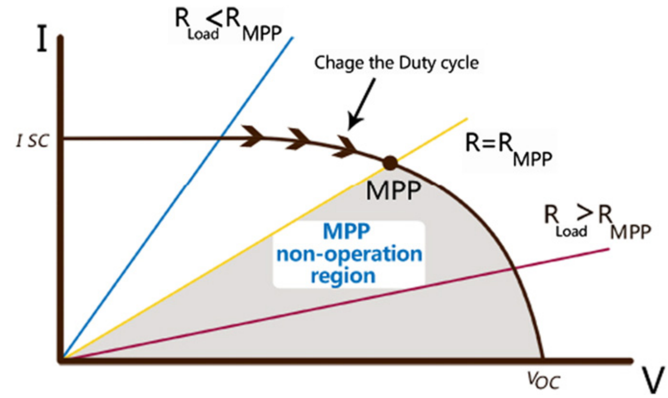

Fig. 4. Operational and non-operational region of *I–V* curve for Boost DC–DC converters.

cannot reflect impedances that are greater than load impedance and therefore does not achieve values near a module's open-circuit voltage [35], i.e., boost converter operates only if $R_{\text{load}} <= R_{\text{mpp}}$.

Fig. 4 shows boost converter not following the curve points that are near the open-circuit voltage, and when the boost converter is used as MPPT, the MPP will be tracked as if it is restricted to within the operation region.

Note that under low irradiation condition, a boost converter cannot track MPP because the point is in the non-operating region.

Many research works have developed applications for DC–DC boost converter in PV systems [51–60]. Li and He reviewed and summarized cost and efficiency of non-isolated DC–DC boost converters of PV and fuel-cell systems. Low-cost and high-efficiency (based on circuit structure) boost converter topologies are [61]:

- Boost converter with coupled inductor,
- Boost converter with switched capacitor,
- Boost converter with inductor and switched capacitor and
- Boost converter with coupled inductor and switched capacitor

Kwon et al. presented a three-phase PV system that has three-level boosting of MPPT control. The three-level boost converter reduces diode reverse recovery losses and reduces input-filter size by canceling input current ripple. The IGBT used in the three-level boost converter has half the rating of that in conventional boost converter. The capacitive turn-on loss is eight times less. Experiment results obtained from a 10-kW prototype showed high performance: wide-ranging PV voltage, high (99.6%) MPPT efficiency, high (96.2%) power conversion efficiency, near-unity power factor, and low (2.0%) Total Harmonic Distortion (THD) of the current [62]. Jung et al. discussed a soft-switching interfaced boost converter of a PV system, and did a numerical analysis of its design. The topology raised efficiency of the DC–DC PV converter and minimized switching losses through the resonant soft-switching. The experiment results for a 1.2 kW prototype converter implied 97.28% efficiency in full-load condition. Consequently, the overall efficiency was confirmed as having increased 1.5% more than achieved by a conventional hard-switching interfaced boost converter [63].

Agorreta et al. proposed placing boost DC–DC converter between PV module and inverter in grid-connected PV system, and use of fuzzy switching technique and cascaded-loop control algorithm for the boost converter, with a new inner-loop strategy that adequately deals with variable operating points, so the DC–DC converter is able to perform in mixed-conduction mode.

The strategy is reliable even if the inductor varied 50% up or down from its nominal value, allowing a wide range of inductor variance [64]. Veerachary et al. developed a feed-forward MPPT for a coupled-inductor interfaced-boost-converter-fed PV system that has a fuzzy controller. It has lower switch-current stress and improved efficiency of non-coupled converter. Depending on the error and changes to the error signals, the fuzzy controller generates a control signal for the PWM generator, adjusting the duty ratio of the converter. The reference voltage corresponding to the MPP of the feed-forward loop is obtained by an offline-trained neural network that uses a back-propagation algorithm [65]. Hsieh et al. used the same DC–DC boost-converter-with-coupled-inductor-and-switched-capacitor technique [66].

Akkaya et al. tested a prototype DSP implementation of a PV system through a genetic-assisted, multi-layer perceptron neural-network-based MPPT controller and a 3-phase brushless DC motor drive that included a DC–DC boost converter. Results acquired in a day with high irradiation show the proposed MPPT controller providing a power increase averaging 25.35%. Also, training the neural network with the genetic-assisted Levenberg–Marquardt algorithm gave better results than did other systems trained by standard gradient-descent algorithms, through less chances of converging to local minima. [67]. Choi et al. presented a new high-gain floating-output boost converter that uses basic non-floating boost and versions of floating boost in PV and fuel-cell systems. The topology offers modularity, lower ripple in both input current and output voltage, and lower voltage and current ratings of the various circuit elements, all as compared with basic boost converter [68].

Elshaer et al. presented a novel smart-PID controller for optimal control of a DC–DC boost converter used as voltage controller in a PV system and which maximizes stable operating range through use of genetic algorithms to tune PID parameters at various loading conditions. Fuzzy logic added intelligence to the controller so it could move among the various PID values. The controller allowed optimal control of the boost converter at any loading condition [69]. Park et al. proposed a soft-switching boost converter; they added a simple auxiliary resonant circuit to a conventional boost converter to improve PV-system energy conversion efficiency. The soft-switching boost converter is easy to control because the same PWM controls the two switches. At turn-on/off, all the switching devices in the converter achieve zero-current switching (ZCS) and zero-voltage switching (ZVS) through the resonant inductor and capacitor. The switching losses dramatically reduced [70].

Bratcu et al. investigated optimization of cascaded DC–DC boost converter for PV system with regard to irradiance conditions and with the advantages of per-panel-converter approach. Such systems can be concluded as guaranteeing good efficiency and rather low cost (both as compared with parallel configurations), mostly because the individual converters are not required to have high boost ratios [71,72]. Rosas-Caro et al. proposed a DC–DC multilevel boost converter that combines the functions of a boost converter and of a switched capacitor to provide various output voltages and a self-balanced voltage. The converter was proposed for use in applications where several controlled voltage levels are needed with self-balancing and unidirectional current flow, such as PV or fuel-cell generation systems [73,74].

Noguchi et al. described a multiple-power-boost-converter system for short-current pulse-based MPPT method. Each module is easily linked parallel to each other on the DC-bus side, and each output power is maximized by individual MPPTs. The system is very flexible in its module connection and highly efficient by its maximized total output power [75].

Pierre Petit et al. designed magnetically coupled coils in a boost converter, which balances the voltage applied to the MOSFET. This topology avoid the over voltage due to the leakage inductor. Then a recovery stage recycling this voltage directly to the output was proposed to add to the earlier converter. This architecture obtain an efficiency of 98.6% for an output power equal to 58 W under an output voltage equal to 180 V [76].

Nejabatkhah et al. proposed a new three-input DC–DC boost converter which applied to hybridize a PV, an FC, and a battery storage system. Four independent duty ratios of the converter facilitate power flow among input sources and the load. Three different power operation modes are defined for the converter and its corresponding transfer function matrix is obtained in each operation mode. The experimental result provides good transient and steady-state responses for the converter with respect to the different step changes in the PV power generation and the load condition [77].

5. Comparing characteristics of buck and boost converters

Buck and boost converters differ in their operational purpose and have individual characteristics. Research works finding the better when buck and boost converters replace each other have been reported. They compared the effect of buck and boost converters on system efficiency, the frequency characteristics of each, component costs, operational conditions, etc.

Xiao et al. investigated PV panel operation in non-ideal conditions and for two topologies with parallel module minimizing performance loss caused by those conditions. They compared the dynamics of the models, frequency characteristics, and component costs, concluded that boost converter's advantages over buck converter are cheaper implementation and better dynamic response, and discussed these:

- Considering the inductor; to achieve the same inductor–current ripple, boost converter needs higher inductance than does buck converter.
- Considering the input capacitors; buck converter needs a large and expensive capacitor to smooth the discontinuous input current of the PV module.
- Considering the power MOSFETs and drivers; the current rating is lower in boost topology. Also, buck converter needs a high-side MOSFET driver, which is more complex and expensive than the low-side driver of boost converter.

In considering the blocking diodes, boost topology shows significant advantages over buck topology. In boost topology, the free-wheeling diode can serve as the blocking diode avoiding reverse current. In the buck interface, however, the blocking diode is an additional component conducting the full PV current [78].

Walker compared buck against boost MPPT topologies and also against direct connection to load battery. On sunny days, the boost and the buck converters performed similarly, and both collected roughly 4% more energy than did direct connection. On cloudy days, buck converter gave the same results as those of direct connection, but boost converter collected about 6% more energy than did the other topologies. Boost converter therefore has slight advantage over buck, mainly at low radiation and because it can constantly track the MPP [79]. Coelho et al. studied the behavior of buck and boost converters in PV system to extract MPP under variations to irradiation and temperature and according to operating and non-operating regions. Their analysis verified that under low irradiation, boost converter cannot track MPP because the point is in the non-operating zone [32,80].

6. DC–DC buck-boost converter

In buck–boost, step-up/down, or bi-directional converters, the output voltage magnitude may be lower or higher than the input voltage magnitude [33], so this topology can be used in connecting nearly-matched battery or load and module voltages. A negative output also results from the common terminal of the input current.

Buck–boost topology can be achieved through cascade connection of the two basic converters (buck converter and boost converter). The output–input voltage conversion ratio is the conversion ratio of the two converters in cascade when the switches in both the converters have the same duty cycle. Buck–boost conversion ratio obtained through buck converter in the first stage results in a buck-boost-cascaded converter. A boost converter in the first stage forms a boost–buck-cascaded converter. The main difference between both configurations is the fewer devices in the buck–boost-cascaded converter [81].

Fig. 5 shows PV module operation point determined by the intersection of the load and generation curves. The resistance conversion ratio of buck–boost converter (see Table 1) shows that increasing D decreases the input impedance R_i thus the PV operating voltage moves to the left region of the *I–V* curve, and that decreasing *D* increases R_i thus the operating voltage moves to the right of the *I–V* curve. Buck-boost converter thus does not have a non-operational zone, so changing the duty cycle enables operation from short-circuit current to open-circuit voltage. The topology is also the only one able to trace the load resistance, which ranges from zero to infinite.

As working in MPP is the main goal of the operation, and the MPP point can be set up anywhere on the *I–V*curve, buck–boost DC–DC converter topology is the only one allowing follow-up of the PV module MPP regardless of temperature, irradiance, and connected load, but the input current of buck–boost topology is always discontinuous (because the switch is in series with the generator), so the current has many harmonic components producing high input ripple and significant noise problems. These converters are thus more complex and expensive [82].

The main disadvantages of this topology are notably high input-voltage ripple and high electrical stresses to the switch [81]. Research works attempting increasing use of buck–boost converters and their control strategy in MPPT systems have been published, as have investigations on how buck–boost converters affect system performance [83–88].

Peftitsis et al. presented a PV array system with a DC–DC buck-boost converter, focusing on the control strategy for the system to operate in MPP and for the converter output voltage to remain constant. They proposed the simplest method of controlling duty cycle *D* and PV array voltage through a new variable $d=D/1-D$; it increases flexibility. A DSP was programmed to provide pulses to the power semiconductor switch of the DC–DC converter for tracking of the PV array MPP [89]. Orellana et al. and Ren et al. suggested use of high-efficiency Four-Switch Buck–Boost (FSBB) structure for PV systems. FSBB has the same voltage step-up/down function as that of traditional buck–boost converter, and has advantages such as positive output and lower voltage stress across the power devices. It has a non-inverted output voltage as in other buck–boost converters [90,91].

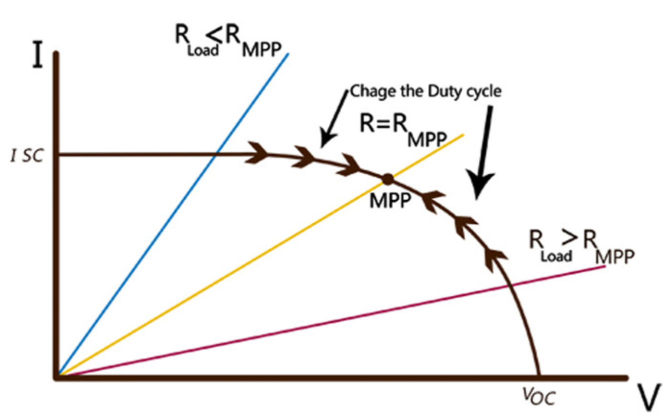

Fig. 5. Operational and non-operational regions of the *I–V* curve for buck–boost, Cúk, and SEPIC DC–DC converters.

Wu et al. demonstrated a fuzzy-logic-controlled single-stage converter (SSC) for PV-powered lighting system. The SSC is an integration of a bidirectional buck–boost charger/discharger. Both fuzzy logic and MPPT control algorithms are implemented in a single-chip microprocessor, simplifying the control circuits and lowering the system cost. Simulation and experiment results verified the feasibility, adaptivity, and robustness of the proposed system [92]. de Britto et al. presented the implementation of a boost–buck quadratic converter with a large input voltage range that can be supplied by a 12 V PV system or the 110 V/220 V of the electricity grid, ideal to drive the LED lamps of private and public lightings. The converter also presents just one switch and only two operation stages. When the converter is supplied by a PV system, the utility-power-grid user saves money. Energy need only be bought when the PV system is under maintenance or when the weather is cloudy [93]. Ic et al. evaluated three direct MPPT algorithms with non-adaptive voltage step for their performance in PV system under dynamic conditions and resistive load. A microcontroller-based buck–boost DC–DC converter platform implemented and compared the algorithms [94].

7. Comparing buck, boost, and buck-boost converters

As with past comparisons between buck and boost converters, surveys to discover the best topology for PV systems from among buck, boost, and buck–boost converters have been done and published.

Enrique et al. sought the best converter configuration for MPPT system from among three basic topologies of DC–DC converters (buck, boost, and buck–boost) with resistive load connected to the PV panels. They drew two fundamental conclusions: one, buck–boost DC–DC converter topology is the only one allowing tracking of PV MPP whatever the temperature, irradiance, and load connection condition, and two, connecting a PV buck–boost DC–DC converter to the PV panel output possibly improves performance. Despite the study being theoretical, buck and boost converters practically are notably the most effective topologies at any price. Its voltage flexibility varies, but buck–boost converter is always either efficiency, or price, disadvantaged [95].

Poshtkouhi et al. compared and analyzed the effectiveness of buck–boost, boost–buck, and boost topologies in PV systems through switching losses, gate-drive losses, and conduction losses of all the components. Fig. 6 gives the efficiency of the three converters versus the current, for a fixed irradiance G_{tot} of 400 W/m^2 and temperature $T=25$ °C. The boost converter yielded 0.3% more energy than did the boost–buck converter for $V_{bus}=280$ V; this, despite its inability to maintain MPPT under all conditions of shade, was owed to its higher efficiency [96,97].

Snyman and Enshn compared the efficiencies of Parallel Power Conversion (PPC), buck, and buck–boost converters. Basic PPC principle was applied to the standard buck topology, changing only the negative terminal connection of the input capacitor. All three converter topologies were evaluated with a 12 V battery and an 18 V array input voltage *V*. The efficiencies differed:

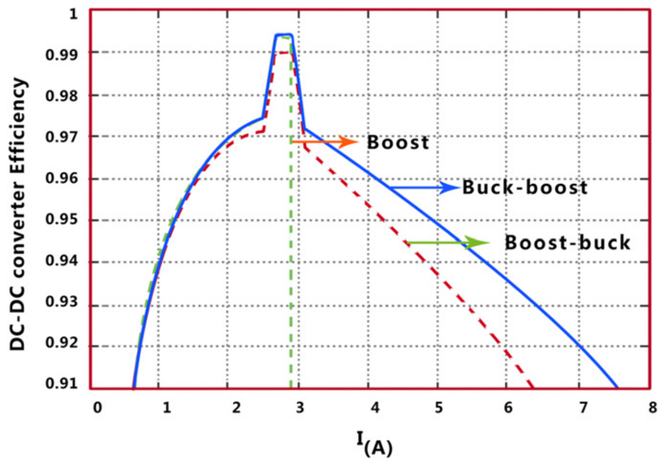

Fig. 6. Efficiencies of buck–boost, boost–buck, and boost converters for G_{tot}=400 W/m^2 and T=25 °C [96].

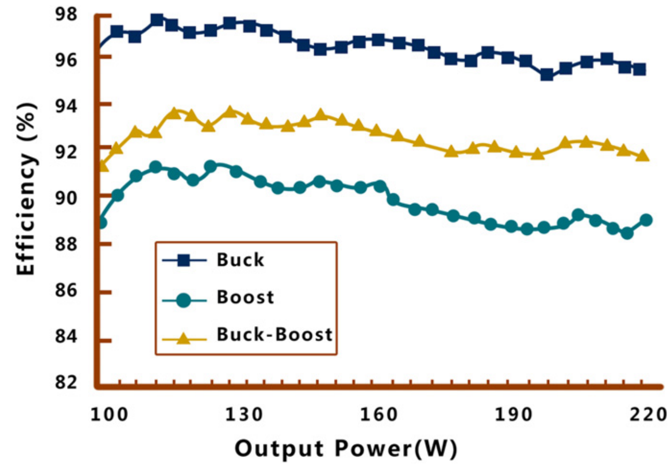

Fig. 8. Efficiencies of DC–DC converters [101,102].

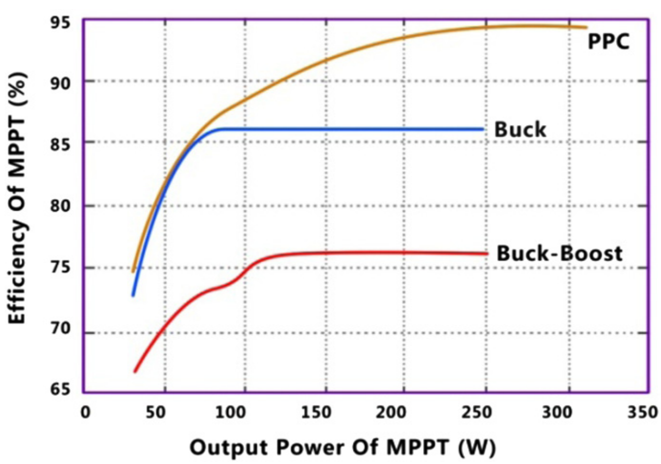

Fig. 7. Comparing the MPPT efficiencies [98–100].

94% for PPC, 86% for buck, and 76% for buck–boost (see Fig. 7) [98–100].

Hua and Shen investigated and compared various MPPT techniques and DC–DC converter (buck, boost, buck–boost) efficiencies in differently-controlled systems. A simple method combining discrete time control and PI compensator tracked the MPPs of the PV panels. Fig. 8 shows efficiency curves versus output powers, for buck, boost, and buck–boost converters. The efficiency of buck converter is a bit higher than that of boost and buck–boost converters [101,102].

Velasquez-Vasquez et al. presented control-oriented models for buck–boost, buck, and boost DC–DC converters. The proposed models have been validated by means of frequency responses of all the states. The applicability of the proposed models was verified by means of experiments performed in a proof of concept PV system based on a boost converter. Such a case was selected because it requires low-side circuitry for driving the Mosfets, which simplify the implementation in comparison to the buck and buck–boost cases. [103]

8. DC–DC cúk converter

Cúk converter is a DC-to-DC converter that performs like buck–boost converter, capable of stepping up or down input voltage with reverse polarity through the common terminal of the input voltage [33]. This topology can be used for connecting nearly-matched battery or load to module voltages.

The operation region of Cúk converter in PV panel is the same as buck–boost converter's (see Fig. 5). Both converters do not have non-operating zone, so changing the duty cycle enables them to operate through short-circuit current to open-circuit voltage. The main difference between Cúk converter and basic DC–DC configurations is the addition of a capacitor and an inductor (see Table 1d). Inductor L1 filters the DC input (to prevent large harmonics) and capacitor C1 is the energy-transfer device (unlike inductor in the basic configurations).

An important advantage of this topology is the continuous current at the converter input and output; the sweep of the *I–V* characteristic is thus more reliable and the converter is less noisy [82]. Disadvantages of the Cúk converter are the high number of passive components and high electrical stresses on the switch, diode, and capacitor C1.

Among converter topologies, Cúk topology has intensively progressed. Many researchers have focused on it [104–108] for maximum power extraction from PV panels through various algorithms such as fuzzy-logic control, direct control, etc.

Safari and Mekhilef used DC–DC Cúk converter to extract MPP from PV system by direct-control method. The main difference of the proposed system to existing MPPT systems includes elimination of the proportional–integral control loop and investigation of the effect of simplifying the control circuit. A DSP controlled the switching of the IGBTs [109]. Bae and Kwasinski proposed multiple-input Cúk DC–DC converter for MPPT to extract maximum power from PV panel in any weather. This method provides current-source interface and is capable of stepping up and down input voltages [110].

Lin et al. presented an integrated Cúk-forward converter in a PV-based LED lighting system. Power switches in the Cúk converter and ZVS forward converter are integrated for fewer components, and synchronous switch in the circuit reduced conduction losses and increased circuit efficiency. Active-clamping technique realized ZVS turn-on of all the switches [111]. Chung et al. presented a novel technique for effective extraction of maximum output power from a solar panel in various weathers. This method connects a PWM DC–DC SEPIC or Cúk converter with a solar panel and a load or a battery bus. The converter operates in discontinuous capacitor voltage mode whereas its input current is continuous. The nominal duty cycle of the main switch in the converter is adjusted to a value at which the converter input resistance equaled the equivalent output resistance of the solar panel at MPP. This approach ensures

maximum power transfer in all weather and no use of microprocessors for calculation [112].

Jiménez-Toribio et al. demonstrated MPPT in a separately-excited DC motor fed by PV panels through Cúk and SEPIC converters. Linear Reoriented Coordinate Method determined the optimal voltage of the PV panels [113]. CRathge and Mecke proposed a high-efficiency Cúk converter topology for interfacing the PV and the battery storage, converting the variable output voltage (60VDC–90VDC) of the storage components into constant DC voltage of up to 650 V. An essential problem is the voltage peaks in the IGBT during switch-off instants considerably exceeding the maximum blocking voltage of the power semiconductor devices. The problem was solved by a special snubber circuit [114].

Mahmoud et al. simulated and implemented a fuzzy-logic controller for a Cúk converter in a standalone PV system. The experiment-built system was validated by comparing the output voltage with and without Cúk converter, and through MMP-matched and non-MPP-matched resistive loads [115].

9. DC–DC sepic converter

Single-Ended Primary Inductor Converter (SEPIC) is a kind of buck-boost converter capable of stepping up or down input voltage and belonging to the class of converter that has two inductors. It has the non-inverting characteristic of buck-boost converters. SEPIC converter, as does Cúk converter, has the desirable feature of the switch control terminal being connected to ground; this simplifies the gate-drive circuitry. As Table 1.e shows, the converter operates via capacitive (C1) and inductive (L1) energy transfer, so voltage stresses in C1 is lower than those in Cúk converter. The converter also has non-pulsating input current [33,34].

The input currents of the Cúk and SEPIC topologies are continuous, and they can draw ripple-free current from a PV panel; this is important for effective MPPT. SEPIC topology, however is notably only applicable to applications where the battery voltage is higher than the PV module voltage [116]. The principle of SEPIC converter is based on buck–boost converter, so their characteristics are the same. SEPIC converter, too, thus does not have a non-operating region in the PV panel (see Fig. 5).

Lin and Huang discussed integrated SEPIC forward converter that uses synchronous switching technique for a PV-based LED lighting system. In charging mode and during daytime, the SEPIC converter delivers solar energy to the battery bank via PV cell modules. At night and in discharging mode, soft-switching forward converter drives the LED lighting system [117].

Veerachary demonstrated voltage-based power tracking of nonlinear PV sources through coupled-inductor SEPIC converter, which was capable of reducing array current ripple and improving converter efficiency. The proposed algorithm was implemented in real-time, aided by ADMC-401 DSP evaluation module analog device. A tracking program was developed for an experiment with analog-to-digital converter (ADC) interrupt. The processor enabled tracking of the maximum power within 200 ms [118].

Duran et al. exemplified the methodology and an experimental system based on interfaced SEPIC converters for measuring *I–V* and *P–V* curves of PV modules. To reduce curve ripple, four parallel-connected SEPIC converters and interleaved operation mode were used. The new development provided a new level of speed, portability, and ease of measurement of peak power, in both the modules and the PV arrays [119].

dos Santos et al. presented the computer simulations of a proposed system of integration of energy sources in which Triple Active Bridge (TAB) converter served as interface. The system had a load, a main voltage source, and an auxiliary power source formed by a PV panel and a SEPIC converter. The TAB converter was fed voltage, and it applied a method of decoupling loops for control of the voltage. The proposed system is applicable to UPS and micro-grids [120]. Huang-Jen Chiu et al. presented a high-intensity-discharge street-lighting PV system with a SEPIC converter for MPPT and battery charging. The converter has high conversion efficiency and shows high MPPT accuracy in various weathers. A SEPIC power-factor correction converter draws energy from the ac-line utility, preventing over-discharging of the battery. Experiment results of a laboratory prototype verified the feasibility of the proposed method [121].

Chiang et al. presented a PV battery charger implemented with a SEPIC converter. The SEPIC design used peak-current-mode control with the current command generated from the input PV voltage regulating loop, where the voltage command was determined by both the PV module MPPT control loop and the battery-charging loop.

Comparison of various buck–boost converters (see Table 2) through various points of view shows that among these converters, though SEPIC is not the best in terms of efficiency and cost, it still has the merits of non-inverting polarity, easy-to-drive switch, and low input-current pulsation for a high-precision MPPT that makes its integral characteristics suitable for low-power PV charger systems [116].

Tse et al. presented a novel technique for efficiently extracting maximum output power from a solar panel. A PWM DC–DC SEPIC or Cúk converter operating in discontinuous inductor–current mode or capacitor–voltage mode matched the output resistance of the panel by injecting the switching frequency with a small sinusoidal-signal variation. The tracking capability was verified by an experiment with a 10 W solar panel [122].

Chen et al. In order to obtain the high efficient solar cell energy conversion, using SEPIC converter circuit board and implemented the fuzzy control strategy with the dsPIC30F4011 control chip [123].

10. Comparing main types of non-isolated converters

As mentioned, buck, boost, buck–boost Cúk and SEPIC converters are classified as main non-isolated converters in PV application.

Table 2
Comparing various buck–boost converters [103].

	Converter			
	Buck-Boost	Cúk	Positive buck–boost	SEPIC
Output voltage polarity	Invert	Invert	Non-invert	Non-invert
Input current	Pulsating	Non-pulsating	Depends o operation mode	Non-pulsating
Switch drive	Floated	Floated	One floated one grounded	Grounded
Efficiency	low	medium	High with only one stage active	Medium
Cost	Medium due to float drive	Medium due to additional block capacitor	High due to an additional switch and diode, a more complex drive circuit	Medium due to additional block capacitor

Each converter topology has some specific characteristics in terms of efficiency, tracking capability, cost, etc. This section presents some reviews that compared various converter topologies.

Farahat et al. investigated the effect of changing cell temperature and solar irradiance on choice and design of various non-isolated topologies of DC–DC converter in PV systems. Shown was that when the duty cycle changes with climate changes, the boundary of the converter design parameters, too, changes. The design parameters must thus be chosen for the highest performance. The study concluded that only buck–boost and Cúk converters are capable of achieving optimal operation whatever the load value. For permanent operation in continuous conduction mode (CCM), the filter inductance of all the converter topologies must be greater than the maximum value of the boundary inductance. Also, to limit to below a specific value the output voltage ripple, the filter capacitance must be larger than the maximum value of the boundary capacitance [124].

Tse et al. presented a comparative study of PV-panel MPPTs that uses Switching-Frequency Modulation Scheme (SFMS). The tracking capability of buck, boost, buck–boost, Cúk, and SEPIC were compared. Authors categorize performance of converters under Discontinuous Inductor Current Mode (DICM) and Discontinuous Capacitor Voltage Mode (DCVM). The study showed the input current ripple in DCVM to be smaller than that in DICM. Variation of the panel-converter operating point in DCVM is thus smaller than in DICM. Also, for the same panel and voltage conversion ratio, the voltage stress on the switch in DCVM is higher than that in DICM. Conversely with the same panel, the current stress in DICM is higher than that in DCVM. For the same panel, DICM is thus more suitable for panels in series connection whereas DCVM better suits parallel connection [125]. Figs. 9 and 10 compare the tracking capability of the converters according to DICM and DCVM.

Walker and Sernia proposed an alternative topology of non-isolated per-panel DC–DC converter connected in series to create a high-voltage string connected to a simplified DC/AC inverter. Buck, boost, buck–boost, and Cúk converters were considered as DC–DC converters that could be cascaded. Fig. 11 shows theoretically calculated efficiencies of four DC–DC converter configurations: buck, boost, buck–boost, and Cúk. For a given cost, buck, followed by boost, converters, are the most effective topologies, with buck best suiting long strings and boost, short strings. For flexibility in voltage ranges, buck–boost and Cúk converters are always either efficiency, or cost, disadvantaged [126].

Dehbonei et al. comprehensively compared Parallel Power Processing (PPP) and Direct Energy Transfer (DET) schemes in DC–DC converters for PV systems. DET was shown to be the key

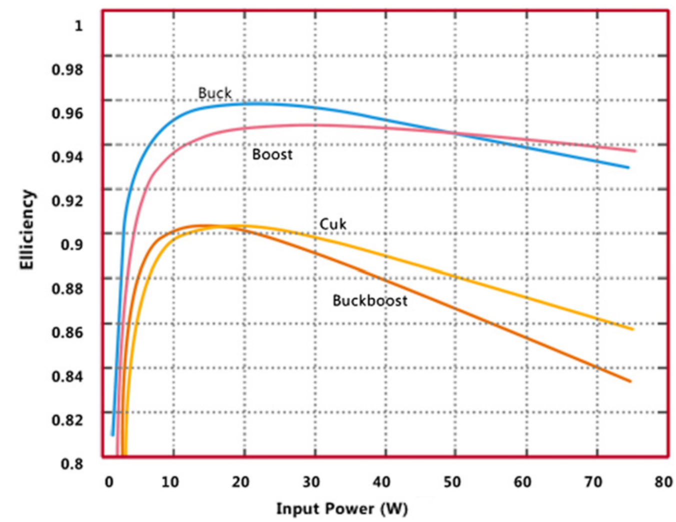

Fig. 11. Theoretically calculated efficiencies of four DC–DC converter configurations: buck, boost, buck–boost, Cúk [126].

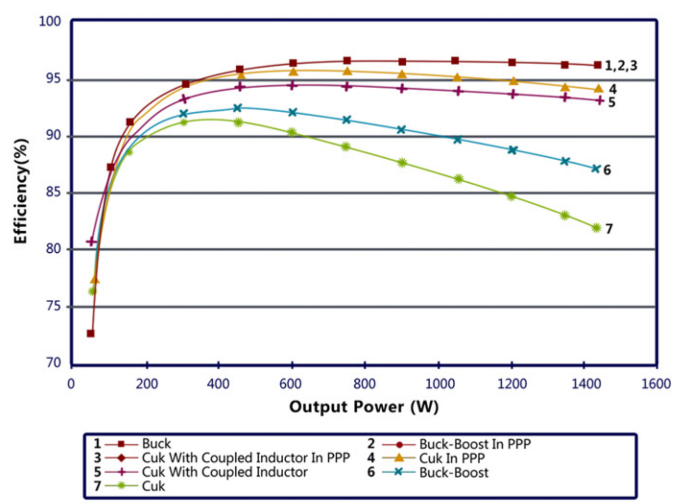

Fig. 12. Efficiency of various DC–DC converters in normal and PPP operations [127,128].

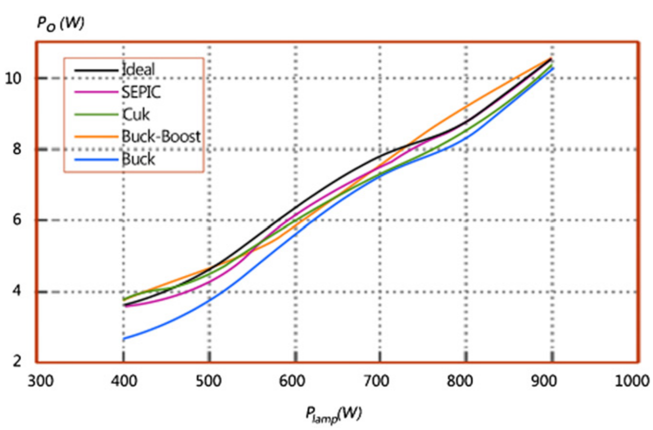

Fig. 9. Comparing the tracking capabilities of the converters in DICM [125].

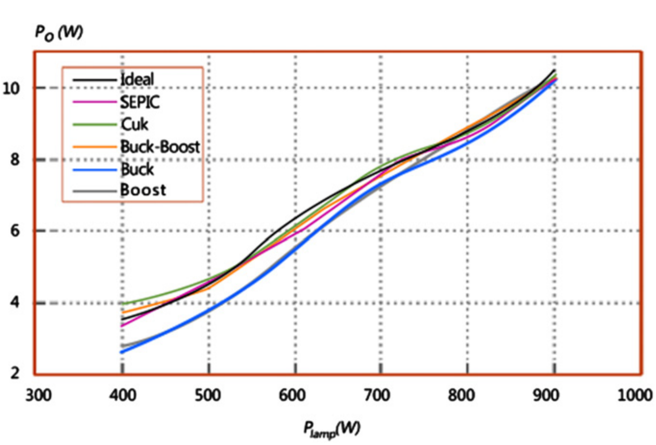

Fig. 10. Comparing the tracking capabilities of the converters in DCVM [125].

increaser of DC–DC converter performance. PPP can provide DET to those DC–DC converters suffering from little or no DET in their turn-on/off modes of operation. It can lead to even higher DET in those converters that had already benefited from DET in their turn on and/or turn off modes of operation (e.g., Cúk with a coupled inductor). A coupling inductor was shown to provide DET to Cúk converter at various modes of operation, but was not as effective as PPP.

To better compare various DC–DC converters and their performance, the efficiency curves of the converters are graphed. Fig. 12 shows the efficiency of various DC–DC converters, in normal operation and in PPP operations. This study showed 96.2% highest efficiency rate to be obtainable from a buck, buck–boost in PPP, or Cúk with coupled inductor in PPP. The other DC–DC converters performed lower: 94% (Cúk with PPP), 93.1% (Cúk with coupled inductor), 87.2% (buck–boost), and 82% (standard Cúk) [127,128].

Thomas Bennett et al. investigated the effect of modeling base on ideal or nonideal buck, boost, buck–boost and Cúk converters.it could be seen that with these small differences in modeling, some significant differences in the dynamic behavior of the converter systems. On the other hand, the converters used with the models should realistically have some nonidealities which could potentially smooth out some differences. This would then seem to indicate that converter systems need not be built dependent on the modules being used in the system. [129]

11. Conclusion

Maximizing energy generation from solar energy has become highly interested. One popular way to maximize the PV generation is use of MPPT and DC–DC converter. In order to help researcher to be able to choose the best converter for their under-studied system, this paper has concisely reviewed various non-isolated DC–DC converters.

Optimal operating performances by different converter topologies are one of the main points which can be summarized. The buck converter should be used with load impedance close to but less than R_{MPP} at the highest condition. However, the boost converter must be used with load impedance close to but larger than R_{MPP} at lowest condition, with a drawback of poor tracking behavior under low radiation. Only the buck–boost, CÚK and SEPIC converters are reviewed to be capable of achieving optimal operation regardless of the load values.

The next point, in term of efficiency, the Buck and Boost converters are the most efficient topologies for a given price. However, they have tracking problems under different connected load, radiation and temperature combinations. In addition, the Buck–Boost, Cúk and SEPIC converters are ideal to MPPT applications, due to their operations are independent from radiation and temperature which allow them track maximum point.

Besides that, the Cúk and SEPIC converters have the highest values of reactive component, which contribute to their main drawback. Although they operate with the best efficiency, alternatively, high cost may become their main disadvantage.

This review paper concludes that the best type of converter for PV system is the buck–boost DC/DC converter. This converter should be able to ensure optimum MPPT operation for any solar irradiation, cell temperature and load conditions.

Efforts continue to make converter and control schemes more efficient and cost effective, aiming for an economically viable solution to increasing concern over environmental issues. Solar power generation has tremendously grown in the past decade, and will continue to do so as power electronic technology continues to advance.

References

[1] Valkila N, Saari A. Urgent need for new approach to energy policy: the case of Finland. Renewable and Sustainable Energy Reviews 2010;14:2068–76.
[2] Olejarnik P. World energy outlook. Paris, France: International Energy Agency; 2010.
[3] Chang J, et al. A review on the energy production, consumption, and prospect of renewable energy in China. Renewable and Sustainable Energy Reviews 2003;7:453–68.
[4] Abbasi T, Abbasi SA. Decarbonization of fossil fuels as a strategy to control global warming. Renewable & Sustainable Energy Reviews 2011;15:1828–34.
[5] Abbasi T, et al. The return to renewables: will it help in global warming control? Renewable & Sustainable Energy Reviews 2011;15:891–4.
[6] Huang Y, Wu JH. Technological system and renewable energy policy: a case study of solar photovoltaic in Taiwan. Renewable and Sustainable Energy Reviews 2007;11:345–56.
[7] Hernandez JA, et al. Analysis of the effect of the implementation of photovoltaic systems like option of distributed generation in Colombia. Renewable & Sustainable Energy Reviews 2011;15:2290–8.
[8] Figueres E, et al. Sensitivity study of the dynamics of three-phase photovoltaic inverters with an LCL grid filter. IEEE Transactions on Industrial Electronics 2009;56:706–17.
[9] Li Q, Wolfs P. A review of the single phase photovoltaic module integrated converter topologies with three different DC link configurations. IEEE Transactions on Power Electronics 2008;23:1320–33.
[10] Li W, He X. Review of non-isolated high step-up DC/DC converters in photovoltaic grid-connected applications. IEEE Transactions on Industrial Electronics 2011:1.
[11] Dincer F. The analysis on photovoltaic electricity generation status, potential and policies of the leading countries in solar energy. Renewable & Sustainable Energy Reviews 2011;15:713–20.
[12] Salas V, Olias E. Overview of the photovoltaic technology status and perspective in Spain. Renewable and Sustainable Energy Reviews 2009;13: 1049–57.
[13] Eltawil MA, Zhao Z. Grid-connected photovoltaic power systems: technical and potential problems–A review. Renewable and Sustainable Energy Reviews 2010;14:112–29.
[14] Mousazadeh H, et al. A review of principle and sun-tracking methods for maximizing solar systems output. Renewable & Sustainable Energy Reviews 2009;13:1800–18.
[15] Abu-Khader MM, et al. Evaluating multi-axes sun-tracking system at different modes of operation in Jordan. Renewable & Sustainable Energy Reviews 2008;12:864–73.
[16] Messenger R, Ventre J. Photovoltaic systems engineering. Boca Raton: CRC Press; 2004.
[17] Gules R, et al. A maximum power point tracking system with parallel connection for PV stand-alone applications,". IEEE Transactions on Industrial Electronics 2008;55:2674–83.
[18] Hohm D, Ropp M. Comparative study of maximum power point tracking algorithms. Progress in photovoltaics: Research and Applications 2003;11: 47–62.
[19] Hussein KH, et al. Maximum photovoltaic power tracking: an algorithm for rapidly changing atmospheric conditions. IEE Proceedings on Generation, Transmission and Distribution 1995;142:59–64.
[20] Kazmi SM Raza , et al. Review and critical analysis of the research papers published till date on maximum power point tracking in wind energy conversion system. In: Proceedings of the 2010 IEEE energy conversion congress and exposition (ECCE); 2010. pp. 4075–4082.
[21] Kjaer SB, et al. Power inverter topologies for photovoltaic modules-a review. In: Proceedings of the 37th IAS annual meeting conference record of the industry applications conference, vol. 2; 2002, pp. 782–788.
[22] Marwan M. Transient analysis of a PV power generator charging a capacitor for measurement of the I–V characteristics. Renewable Energy 2006;31:2198–206.
[23] Muñoz J, Lorenzo E. Capacitive load based on IGBTs for on-site characterization of PV arrays. Solar Energy 2006;80:1489–97.
[24] Kuai Y, Yuvarajan S. An electronic load for testing photovoltaic panels. Journal of Power Sources 2006;154:308–13.
[25] Forero N, et al. Development of a monitoring system for a PV solar plant. Energy Conversion and Management 2006;47:2329–36.
[26] Malik AQ, Damit SJBH. Outdoor testing of single crystal silicon solar cells. Renewable Energy 2003;28:1433–45.
[27] Fernández-Reche J, et al. PSA Solar furnace: a facility for testing PV cells under concentrated solar radiation. Solar Energy Materials and Solar Cells 2006;90:2480–8.
[28] de Blas MA, et al. Selecting a suitable model for characterizing photovoltaic devices. Renewable Energy 2002;25:371–80.
[29] Recart F, et al. Simple data acquisition of the current–voltage and illumination-voltage curves of solar cells. In: Proceedings of the IEEE 4th world conference record of the photovoltaic energy conversion; 2006. pp. 1215–1218.
[30] Guvench MG, et al.. Solar simulator and *I–V* measurement system for large area solar cell testing. In: Proceedings of the 2004 american society for engineering education annual conference & exposition. 2004.
[31] van Dyk EE, et al. Monitoring current–voltage characteristics and energy output of silicon photovoltaic modules. Renewable Energy 2005;30: 399–411.

[32] Coelho RF, et al. A study of the basic DC–DC converters applied in maximum power point tracking. In: Proceedings of the power electronics conference, COBEP '09, Brazilian; 2009. pp. 673–678.
[33] Rashid MH. Power electronics handbook. Academic Press; 2001.
[34] Mohan NT, Undeland M, Robbins WP. Power electronics: converters, applications and design. 3rd ed. John Wiley & Sons: New york; 2004.
[35] Enrique JM. et al. A new approach to obtain I–V and P–V curves of photovoltaic modules by using DC-DC converters. In: Photovoltaic Specialists Conference, 2005. Conference Record of the Thirty-first IEEE, Florida, 2005, pp. 1769–1772.
[36] Solodovnik EV, et al. Power controller design for maximum power tracking in solar installations. IEEE Transactions on Power Electronics 2004;19: 1295–304.
[37] Femia N, et al. Optimized one-cycle control in photovoltaic grid connected applications. IEEE Transactions on Aerospace and Electronic Systems 2006;42: 954–72.
[38] Ilango GSaravana, et al. Single-stage sine-wave inverter for an autonomous operation of solar photovoltaic energy conversion system. Renewable Energy 2010;35:275–82.
[39] Masoum MAS, et al. Microprocessor-controlled new class of optimal battery chargers for photovoltaic applications. IEEE Transactions on Energy Conversion 2004;19:599–606.
[40] Elgendy MA, et al. Assessment of perturb and observe MPPT algorithm implementation techniques for PV pumping applications. IEEE Transactions on Sustainable Energy 2012;3:21–33.
[41] Mazouz N, Midoun A. Control of a DC/DC converter by fuzzy controller for a solar pumping system. International Journal of Electrical Power & Energy Systems 2011.
[42] Koutroulis E, et al. Development of a microcontroller-based, photovoltaic maximum power point tracking control system. IEEE Transactions on Power Electronics 2001;16:46–54.
[43] Chian-Song C. T–S fuzzy maximum power point tracking control of solar power generation systems. IEEE Transactions on Energy Conversion 2010;25:1123–32.
[44] Chew KWR, Siek L.Single inductor quad-input-dual-output buck converter for photovoltaic systems. In: Proceedings of the IECON 2010 – 36th annual conference on IEEE industrial electronics society; 2010. pp. 704–709.
[45] Longlong Z, et al. A new approach to achieve maximum power point tracking for PV system with a variable inductor. IEEE Transactions on Power Electronics 2011;26:1031–7.
[46] Veerachary M. Fourth-order buck converter for maximum power point tracking applications. IEEE Transactions on Aerospace and Electronic Systems 2011;47:896–911.
[47] Yang D, et al. One-cycle control for double-input DC/DC converter. IEEE Transactions on Power Electronics 2011:1.
[48] Villalva MG, et al. Voltage regulation of photovoltaic arrays: small-signal analysis and control design. IET Power Electronics 2010;3:869–80.
[49] Pernía AM, et al. A modular strategy for isolated photovoltaic systems based on microcontroller. Renewable Energy 2009;34:1825–32.
[50] Taufik AO, et al. Modeling and simulation of photovoltaic water pumping system. In: Proceedings of the third asia international conference on modelling & simulation, AMS '09; 2009. pp. 497–502.
[51] Santos JL, et al. A maximum power point tracker for PV systems using a high performance boost converter. Solar Energy 2006;80:772–8.
[52] Nejabatkhah F, et al. Modeling and control of a new three-input DC–DC boost converter for hybrid PV/FC/battery power system. IEEE Transactions on Power Electronics 2011:1.
[53] Benavides ND, Chapman PL. Modeling the effect of voltage ripple on the power output of photovoltaic modules. IEEE Transactions on Industrial Electronics 2008;55:2638–43.
[54] Du Y, Lu DD-C. Battery-integrated boost converter utilizing distributed MPPT configuration for photovoltaic systems. Solar Energy 2011;85: 1992–2002.
[55] Park S-J, et al. New parallel driving strategy based on modified converters and peak current mode control for photovoltaic power generation systems. Solar Energy 2006;80:524–34.
[56] Femia N, et al. Optimization of perturb and observe maximum power point tracking method. IEEE Transactions on Power Electronics 2005;20:963–73.
[57] Kottas TL, et al. New maximum power point tracker for PV arrays using fuzzy controller in close cooperation with fuzzy cognitive networks. IEEE Transactions on Energy Conversion 2006;21:793–803.
[58] Bandyopadhyay S, Chandrakasan AP. Platform architecture for solar, thermal, and vibration energy combining with MPPT and single inductor. IEEE Journal of Solid-State Circuits 2012:1–17.
[59] Kadri R, et al. Nondissipative string current diverter for solving the cascaded DC–DC converter connection problem in photovoltaic power generation system. IEEE Transactions on Power Electronics 2012;27: 1249–58.
[60] Park J, Kim S. Maximum power point tracking controller for thermoelectric generators with peak gain control of boost DC–DC converters. Journal of Electronic Materials 2012:1–5.
[61] Wuhua L, Xiangning H. Review of nonisolated high-step-up DC/DC converters in photovoltaic grid-connected applications. IEEE Transactions on Industrial Electronics 2011;58:1239–50.
[62] Kwon JM, et al. Three-phase photovoltaic system with three-level boosting MPPT control. IEEE Transactions on Power Electronics 2008;23:2319–27.
[63] Doo-Yong J, et al. Interleaved soft-switching boost converter for photovoltaic power-generation system. IEEE Transactions on Power Electronics 2011;26:1137–45.
[64] Agorreta JL, et al. Fuzzy switching technique applied to PWM boost converter operating in mixed conduction mode for PV systems. IEEE Transactions on Industrial Electronics 2009;56:4363–73.
[65] Veerachary M, et al. Neural-network-based maximum-power-point tracking of coupled-inductor interleaved-boost-converter-supplied PV system using fuzzy controller. IEEE Transactions on Industrial Electronics 2003;50:749–58.
[66] Yi-Ping H, et al. Novel high step-up DC–DC converter with coupled-inductor and switched-capacitor techniques,''. IEEE Transactions on Industrial Electronics 2012;59:998–1007.
[67] Akkaya R, et al. DSP implementation of a PV system with GA-MLP-NN based MPPT controller supplying BLDC motor drive. Energy Conversion and Management 2007;48:210–8.
[68] Choi S, et al. Analysis, design and experimental results of a floating-output interleaved-input boost-derived DC–DC high-gain transformer-less converter. IET Power Electronics 2011;4:168–80.
[69] Elshaer M, et al. Smart optimal control of DC–DC boost converter in PV systems. In: Transmission and distribution conference and exposition, Latin America (T&D-LA), 2010 IEEE/PES; 2010. pp. 403–410.
[70] Sang-Hoon P, et al. Design and application for PV generation system using a soft-switching boost converter with SARC,''. IEEE Transactions on Industrial Electronics 2010;57:515–22.
[71] Bratcu AI, et al. Cascaded DC–DC converter photovoltaic systems: power optimization issues. IEEE Transactions on Industrial Electronics 2011;58:403–11.
[72] Bratcu AI, et al. Power optimization strategy for cascaded DC–DC converter architectures of photovoltaic modules. In: Proceedings of the IEEE international conference on industrial technology, ICIT; 2009. pp. 1–8.
[73] Rosas-Caro JC, et al. A DC–DC multilevel boost converter. IET Power Electronics 2010;3:129–37.
[74] Mayo-Maldonado JC, et al. Modelling and control of a DC–DC multilevel boost converter. IET Power Electronics 2011;4:693–700.
[75] Noguchi T, et al. Short-current pulse-based maximum-power-point tracking method for multiple photovoltaic-and-converter module system. IEEE Transactions on Industrial Electronics 2002;49:217–23.
[76] Petit P, et al. New architecture for high efficiency DC–DC converter dedicated to photovoltaic conversion. Energy Procedia 2011;6:688–94.
[77] Nejabatkhah F, et al. Modeling and control of a new three-input DC–DC boost converter for hybrid PV/FC/battery power system. IEEE Transactions on Power Electronics 2011:1.
[78] Xiao WD, et al. Topology study of photovoltaic interface for maximum power point tracking. IEEE Transactions on Industrial Electronics 2007;54: 1696–704.
[79] Walker G. Evaluating MPPT converter topologies using a matlab pv model. Journal of Electrical Electronics Engineering 2001;21.
[80] Coelho RF, et al. Analytical and experimental analysis of DC–DC converters in photovoltaic maximum Power Point Tracking applications. In: Proceedings of the IECON 2010 – 36th annual conference on IEEE industrial electronics society; 2010. pp. 2778–2783.
[81] Duran E, et al. Comparative analysis of buck-boost converters used to obtain *I–V* characteristic curves of photovoltaic modules. In: Proceedings of the IEEE power electronics specialists conference, PESC; 2008. pp. 2036–2042.
[82] Durán E, et al. A high-flexibility DC load for fuel cell and solar arrays power sources based on DC–DC converters. Applied Energy 2011;88:1690–702.
[83] Zegaoui A, et al. Dynamic behaviour of PV generator trackers under irradiation and temperature changes. Solar Energy 2011;85:2953–64.
[84] Chakraborty S, et al. A review of power electronics interfaces for distributed energy systems towards achieving low-cost modular design. Renewable and Sustainable Energy Reviews 2009;13:2323–35.
[85] Veera CM. Steady-state and dynamic performance analysis of PV supplied DC motors fed from intermediate power converter. Solar Energy Materials and Solar Cells 2000;61:365–81.
[86] Patel H, Agarwal V. A single-stage single-phase transformer-less doubly grounded grid-connected PV interface. IEEE Transactions on Energy Conversion 2009;24:93–101.
[87] Jain S, Agarwal V. A Single-stage grid connected inverter topology for solar PV Systems with maximum power point tracking. IEEE Transactions on Power Electronics 2007;22:1928–40.
[88] Ishaque K, Salam Z. A deterministic particle swarm optimization maximum power point tracker for photovoltaic system under partial shading condition. IEEE Transactions on Industrial Electronics 2012:1.
[89] Peftitsis D, et al. Photovoltaic system MPPTracker investigation and implementation using DSP engine and buck–boost DC–DC converter. In: Proceedings of the power electronics and motion control conference, EPE-PEMC; 2008. pp. 1840–1846.
[90] Orellana M, et al. Four switch buck–boost converter for photovoltaic DC–DC power applications. In: Proceedings of the IECON 2010 36th annual conference on IEEE industrial electronics society; 2010. pp. 469–474.
[91] Xiaoyong R, et al. Three-mode dual-frequency two-edge modulation scheme for four-switch Buck–boost converter. IEEE Transactions on Power Electronics 2009;24:499–509.
[92] Tsai-Fu W, et al. A fuzzy-logic-controlled single-stage converter for PV-powered lighting system applications. IEEE Transactions on Industrial Electronics 2000;47:287–96.

[93] de Britto JR, et al. Proposal of a DC–DC converter with wide conversion range used in photovoltaic systems and utility power grid for the universal voltage range. In: Proceedings of the 2010 twenty-fifth annual IEEE on applied power electronics conference and exposition (APEC); 2010. pp. 2258–2263.
[94] Andrejas, et al. Comparison of direct maximum power point tracking algorithms using EN 50530 dynamic test procedure. IET Renewable Power Generation 2011;5:281–6.
[95] Enrique JM, et al. Theoretical assessment of the maximum power point tracking efficiency of photovoltaic facilities with different converter topologies. Solar Energy 2007;81:31–8.
[96] Poshtkouhi S, et al. A general approach for quantifying the benefit of distributed power electronics for fine grained MPPT in photovoltaic applications using 3D modeling. IEEE Transactions on Power Electronics 2011:1.
[97] Poshtkouhi S, et al. A general approach for quantifying the benefit of distributed power electronics for fine grained MPPT in photovoltaic applications using 3-D modeling. IEEE Transactions on Power Electronics 2012;27:4656–66.
[98] Snyman D, Enslin J. An experimental evaluation of MPPT converter topologies for PV installations. Renewable Energy 1993;3:841–8.
[99] Snyman DB, Enslin JHR. Analysis and experimental evaluation of a new MPPT converter topology for PV installations. In: Proceedings of the 1992 international conference on industrial electronics, control, instrumentation, and automation, power electronics and motion control, vol. 1; 1992. pp. 542–547.
[100] Snyman DB, Enslin JHR. Novel technique for improved power conversion efficiency in systems with battery back-up. Renewable Energy 1994;4: 349–57.
[101] Chihchiang H, Chihming S. Study of maximum power tracking techniques and control of DC/DC converters for photovoltaic power system. In: Proceedings of the 29th annual IEEE power electronics specialists conference, PESC 98 Record, vol. 1; 1998. pp. 86–93.
[102] Chihchiang H, et al. Implementation of a DSP-controlled photovoltaic system with peak power tracking. IEEE Transactions on Industrial Electronics 1998;45:99–107.
[103] Velasquez-Vasquez JC, et al. Control-oriented models of step-up and step-down photovoltaic power systems. Dyna 2012;172:67–76.
[104] Chong B, et al. Optimal design of cuk step-up converter for photovoltaic energy systems. In: Proceedings of the 5th IET international conference on power electronics, machines and drives, PEMD; 2010. pp. 1–6.
[105] Miao Z, et al. Novel cuk circuit and its application in photovoltaic system. In: Proceedings of the 3rd international conference on power electronics systems and applications, PESA; 2009. pp. 1–4.
[106] Wei P, et al. Research on maximum power point tracker based on solar cells simulator. In: Proceedings of the 2nd international conference on advanced computer control, ICACC; 2010. pp. 319–323.
[107] Zengshi C. PI and sliding mode control of a cuk converter. IEEE Transactions on Power Electronics 2012;27:3695–703.
[108] Algazar MM, et al. Maximum power point tracking using fuzzy logic control. International Journal of Electrical Power Energy Systems 2012;39: 21–8.
[109] Safari A, Mekhilef S. Simulation and hardware implementation of incremental conductance MPPT with direct control method using cuk converter. IEEE Transactions on Industrial Electronics 2011;58:1154–61.
[110] Sungwoo B, Kwasinski A. Maximum power point tracker for a multiple-input Ćuk dc–dc converter. In: Proceedings of the 31st international telecommunications energy conference, INTELEC; 2009. pp. 1–5.
[111] Lin BR, et al. Integrated Cuk-forward converter for photovoltaic-based LED lighting. International Journal of Electronics 2009;96:943–59.
[112] Chung HSH, et al. A novel maximum power point tracking technique for solar panels using a SEPIC or Cuk converter. IEEE Transactions on Power Electronics 2003;18:717–24.
[113] Jimenez-Toribio EE, et al. Sensorless control of SEPIC and Ćuk converters for DC motors using solar panels. In: Proceedings of the IEEE international electric machines and drives conference, IEMDC '09; 2009. pp. 1503–1510.
[114] Rathge C, Mecke R Converter for energy storage integration in photovoltaic plants. In: Proceedings of the 2002 IEEE international symposium on industrial electronics, ISIE, vol. 3; 2002. pp. 959–963.
[115] Mahmoud AMA, et al. In: Proceedings of the 26th Annual Confjerence of the IEEE Fuzzy logic implementation for photovoltaic maximum power tracking in industrial electronics society, ECON, vol. 1. 2000. pp. 735–740.
[116] Chiang S, et al. Modeling and control of PV charger system with SEPIC converter. IEEE Transactions on Industrial Electronics 2009;56:4344–53.
[117] Lin BR, Huang CL. Analysis and implementation of an integrated sepic-forward converter for photovoltaicbased light emitting diode lighting. IET Power Electronics 2009;2:635–45.
[118] Veerachary M. Power tracking for nonlinear PV sources with coupled inductor SEPIC converter. IEEE Transactions on Aerospace and Electronic Systems 2005;41:1019–29.
[119] Durán E, et al. Methodology and experimental system for measuring and displaying *I–V* characteristic curves of PV facilities. Progress in Photovoltaics: Research and Applications 2009;17:574–86.
[120] dos Santos WM, et al. Application of the voltage fed TAB converter as energy source coupler. IEEE Latin America Transactions (Revista IEEE America Latina) 2011;9:510–5.
[121] Huang-Jen C, et al. Design and implementation of a photovoltaic high-intensity-discharge street lighting system. IEEE Transactions on Power Electronics 2011;26:3464–71.
[122] Tse K, et al. A novel maximum power point tracker for PV panels using switching frequency modulation. IEEE Transactions on Power Electronics 2002;17:980–9.
[123] Ta-Tau C, et al. Proceedings of the IEEE international conference on design of digital battery charger system based on PV-module in fuzzy systems (FUZZ); 2011. pp. 1860–1865.
[124] Farahat MA, et al. Optimal choice and design of different topologies of DC–DC converter used in PV systems, at different climatic conditions in Egypt. Renewable Energy 2012;43:393–402.
[125] Tse KK, et al. A comparative study of maximum-power-point trackers for photovoltaic panels using switching-frequency modulation scheme. IEEE Transactions on Industrial Electronics 2004;51:410–8.
[126] Walker GR, Sernia PC. Cascaded DC–DC converter connection of photovoltaic modules. IEEE Transactions on Power Electronics 2004;19:1130–9.
[127] Dehbonei H, et al. Direct energy transfer for high efficiency photovoltaic energy systems part i: concepts and hypothesis. IEEE Transactions on Aerospace and Electronic Systems 2009;45:31–45.
[128] Dehbonei H, et al. Direct energy transfer for high efficiency photovoltaic energy systems part ii: experimental evaluations. IEEE Transactions on Aerospace and Electronic Systems 2009;45:46–57.
[129] T. Bennett, et al., Photovoltaic model and converter topology considerations for MPPT purposes Solar Energy, 2012.